Journal of Thermal Analysis and Calorimetry, Vol. 72 (2003) 967–980

THERMAL ANALYSIS OF MECHANOACTIVATED MIXTURES OF TUNISIA PHOSPHORITE AND AMMONIUM SULFATE

Y. Pelovski [1*], *V. Petkova* [2] *and I. Dombalov* [1]

[1]University of Chemical Technology and Metallurgy, 8 Kl. Ohridski Blvd, 1756 Sofia, Bulgaria
[2]Central Laboratory of Mineralogy and Crystallography, Bulgarian Academy of Sciences,
Acad. G. Bonchev St., Bl. 107, 1113 Sofia, Bulgaria

Abstract

The thermal behavior of Tunisia phosphorite and ammonium sulfate mixtures are examined by non-isothermal thermogravimetry in air atmosphere. It has been shown that the thermal stability of mixtures have different behavior after mechano-chemical treatment due to phase changes in the mixtures. New solid phases are confirmed by the stages and rate of mass changes and also by the heat effects observed. New phases are also confirmed by using X-ray diffraction method. Based on the data obtained by the mechanism of chemical transformations is proposed.

The kinetics of mechano-activated mixtures decomposition is significantly influenced by the time of treatment and proceeds in few stages. Stage I is attributed to the effect of partially ammonia releasing, when the next stages are associated with the decomposition of apatite structures. Because of the interfacial interactions during mechano-chemical treatment insoluble phosphorous forms from apatite structures are transformed to the soluble forms suitable for plants nutrition. The results have shown that the soluble form can be controlled by the initial components ratio and conditions of treatment on the way to obtain slow releasing nutrition products.

Keywords: phosphate of ammonium and calcium, solid state reaction, thermal decomposition, tribo-activation

Introduction

Thermo-tribo-chemical method for treatment of raw materials became a new way for processing raw materials with low content of useful components and unsuitable for treatment using traditional technologies. Structure defects, created during activation of solids increases the reactivity of the systems and makes the efficiency higher [1, 2]. Energy accumulated during activation process often is released when temperature rises and the rate of chemical reactions takes place [3–5]. Sometimes the energy released is even higher than needed for certain processes and the optimization of activation conditions is required. Topochemical character of the activated systems decomposition makes the systems unique and concrete studies may describe their behavior.

---

[*] Author for correspondence: E-mail: pelovsky@uctm.edu

1388–6150/2003/ $ 20.00

Akadémiai Kiadó, Budapest
Kluwer Academic Publishers, Dordrecht

Natural phosphate-ammonium sulfate mixtures have been studied as a promising system for fertilizer production [6–11]. Such fertilizers may supply plants with few nutrients – nitrogen, phosphorous, sulfur and calcium. By different chemical and physical methods it is confirmed that different forms of P_2O_5, suitable for assimilation by the plants could be obtained [11]. Thermomechanical activation of the mixtures selected may accelerate the reactions decomposing the insoluble forms of phosphorous from natural phosphates to soluble one and it is the aim of the present work.

Thermochemical reactions take place in the mixtures of Tunisia phosphorite and ammonium sulfate with mass ratio 1:1, activated from 10 min to 50 h in a planetary mill with Cr–Ni milling balls are studied by use of thermal analysis and X-ray diffraction methods.

Methods and raw materials

Tunisia phosphorite contain 29.58 mass% P_2O_5, 48.40 mass% CaO, 6.48 mass% CO_2, 3.58 mass% SO_3, 2.74 mass% F, 1.88 mass% SiO_2, 1.38 mass% Na_2O, 1.07 mass% R_2O_3, 0.07 mass% K_2O, 0.056 mass% Cl and traces of Cd, Pb, Cr, Ni. Ammonium sulfate is p.a. grade from Alerus Ltd. containing 99.5 mass% $(NH_4)_2SO_4$. As impurities 0.001% NO_3^-, 0.0003% Cl^-, 0.0005% PO_4^{3-}, 0.0002% Fe, 0.00002% As and 0.0002% the supplier specifies as other heavy metals.

Pulverisette-5 of Fritsch Ltd. planetary mill with Cr–Ni milling balls (total volume 120 mL; total mass 0.562 kg; number 140) is used for tribo-activation of 0.02 kg samples. For thermal analysis Stanton Redcroft thermal analyzer in temperature range 288–1373 K is used. Heating rate is 10 K min^{-1} and mass of samples is 15.20±0.4 mg. DRON X-ray analyzer with CuK_α radiation is also used.

Results and discussions

Figures 1–6 and Tables 1–4 represent TG-DTA and X-ray diffractograms of the initial reagents and mixture and activated mixtures after different time of treatment. X-ray data for (Fig. 1) identified phase structures in the raw materials and mixture are $Ca_5F(PO_4)_3$, β-$Ca_3(PO_4)_2$, SiO_2 and $(NH_4)_2SO_4$.

Thermal decomposition of ammonium sulfate (AS)

Thermal decomposition of ammonium sulfate is a multistage process (Table 1 and Fig. 2), where the first stage is in the temperature range 543–673 K and from the sample NH_3 is released as a result of transformation to NH_4HSO_4. In the temperature range 723–823 K are the next step reactions where NH_4HSO_4 is partially transformed to $(NH_4)_2S_2O_8$. Last stage is in the temperature range 913–1033 K where full decomposition takes place and only the volatile products are obtained.

Table 1 Mass losses of ammonium sulfate at different stages of decomposition

Stage	Mass losses/%		Stage's mass losses/%	Temperature/K	
	Start	End	–	Start	Endo
I	0.00	16.50	16.50	543.5	386.7
II	16.50	87.55	71.10	659.7	810.0
III	89.45	91.81	2.36	921.2	1026.4
Total mass losses – 93.54%					

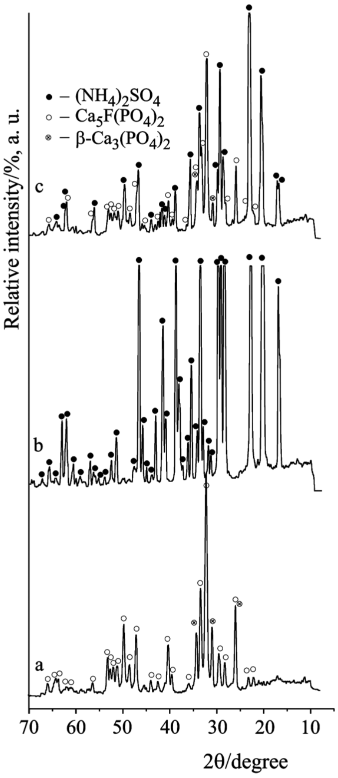

Fig. 1 X-ray diffractograms of the raw materials and mixtures: a – X-ray diffractogram of the raw TPh; b – X-ray diffractogram of the raw AS; c – X-ray diffractogram of the initial mixture mass ratio 1:1

Analysis of the results from TG-DTA curves and X-ray diffraction data show that decomposition process of ammonium sulfate could be described by the following reactions:

Stage I – 543–663 K, 16.5 mass loss/%

$$(NH_4)_2SO_4=NH_4HSO_4+NH_3 \tag{1}$$

$$2(NH_4)_2SO_4=(NH_4)_3H(SO_4)_2+2NH_3 \quad (2)$$

Stage II – 653–813 K, 71.1 mass loss/%

$$(NH_4)_3H(SO_4)_2=2NH_4HSO_4+NH_3 \quad (3)$$

$$(NH_4)_3H(SO_4)_2=(NH_4)_2S_2O_8+NH_3+H_2O \quad (4)$$

$$NH_4HSO_4=NH_3+SO_3+H_2O \quad (5)$$

Stage III – 913–1033 K, 2.4 mass loss/%

$$(NH_4)_2S_2O_8=2NH_3+2SO_3+H_2O+½O_2 \quad (6)$$

$$SO_3=SO_2+½O_2 \quad (7)$$

Thermal behavior of Tunisia phosphorite (TPh)

During thermal treatment of the Tunisia phosphorite up to 1373 K total mass losses are about 12% (Fig. 2, Table 2). Up to 423 K free water and volatile organic impurities are released; in the temperature range 573–923 K oxidation of heavy organic impurities takes place and up to 1223 K the release of carbon dioxide, because of carbonate's impurities decomposition is completed.

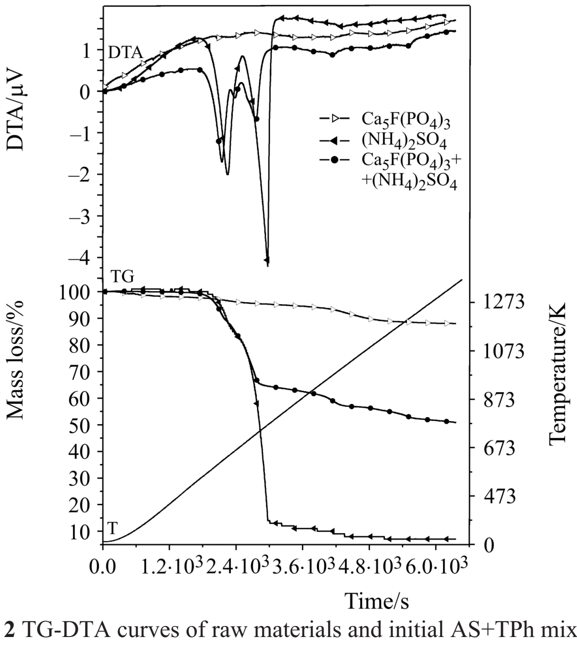

Fig. 2 TG-DTA curves of raw materials and initial AS+TPh mixture

Table 2 Mass losses at different stages during thermal treatment of Tunisia phosphorite

Stage	Mass losses/%		Stage mass losses/%	Temperature/K	
	Start	End	–	Start	End
I	0.00	1.68	1.68	293.0	422.3
II	2.37	5.74	3.37	578.6	927.2
III	5.74	11.28	5.54	927.2	1192.7
Total mass losses – 11.95%					

Untreated mixtures of AS and TPh

Registered mass losses and thermal effects (Fig. 2, Table 3) confirmed complicated mechanism of transformation, related from one side to the individual behavior of the main components and to the reactions between from the other side. As it was confirmed in the other papers [6–11] some of the released intermediates, like NH_4^+, SO_3, take part in a secondary reactions and new solid phases are confirmed in the final product, like orto- or polyphosphates of ammonia and calcium. Mass losses registered correspond well with the step-by-step formation of $(NH_4)_2SO_4{\cdot}2CaSO_4$, $CaHPO_4$, $NH_4CaP_3O_9$, α-$Ca_2P_2O_7$, $Ca_3(PO_4)_2$, $CaSO_4$. Formation of $CaHPO_4$ may come on the base of the reaction between $Ca_5F(PO_4)_3$ and the intermediate acidic phase NH_4HSO_4, formed during first stage of AS decomposition. $NH_4CaP_3O_9$, α-$Ca_2P_2O_7$, $Ca_3(PO_4)_2$ and $CaSO_4$ appear at higher temperatures as a result of dehydration and polymerization of the phosphate complex and $CaSO_4$. Welsh [6] stated that $NH_4CaP_3O_9$ decomposes to $(NH_4)_2P_2O_6$ and CaP_2O_6, but the mass losses registered are closer to the transformation of $NH_4CaP_3O_9$ to α-$Ca_2P_2O_7$. On the basis of our studies we suppose that in the temperature range 293–1373 K chemical mechanisms of transformations in the AS–TPh mixture can be described by the following reactions:

523–643 K, 11.75 mass loss/%

$$(NH_4)_2SO_4=NH_4HSO_4+NH_3 \quad (1)$$

$$2(NH_4)_2SO_4=(NH_4)_3H(SO_4)_2+2NH_3 \quad (2)$$

633–673 K, 5.43 mass loss/%

$$2Ca_5F(PO_4)_3+(NH_4)_2SO_4=3Ca_3(PO_4)_2+CaSO_4+2HF+2NH_3 \quad (8)$$

$$Ca_5F(PO_4)_3+3NH_4HSO_4=(NH_4)_2SO_4{\cdot}2CaSO_4+3CaHPO_4+HF+NH_3 \quad (9)$$

673–708 K, 9.92 mass loss/%

$$(NH_4)_2SO_4{\cdot}2CaSO_4=NH_4HSO_4+2CaSO_4+NH_3 \quad (10)$$

$$3CaHPO_4+2NH_4HSO_4=NH_4CaP_3O_9+2CaSO_4+NH_3+3H_2O \quad (11)$$

$$2CaHPO_4=Ca_2P_2O_7+H_2O \quad (12)$$

Table 3 Mass losses and temperature ranges for initial components and activated AS+TPh mixture in the planetary mill; time of activation –0.12–50 h

Time of activation/h	Stage I		Stage II		Stage III		Stage IV	
	Temperature range/K	Mass loss/%	Temperature range/K	Mass loss/%	Temperature range/K	Mass loss/%	Temperature range/K	Mass loss/%
0.00	–	–	–	–	531.5–634.7 infl. p.–607.6	11.75	634.7–670.7 infl. p.–649.7	5.34
0.12	303.1–363.2 infl. p.*–332.1	1.51	423.3–493.4 infl. p.–464.4	0.88	493.4–562.5 infl. p.–544.5 562.5–644.7 infl. p.–588.8	3.61 10.09	–	–
0.50	301.1–363.2 infl. p.–328.1	4.01	434.3–495.4 infl. p.–464.4	1.05	495.4–564.5 infl. p.–552.5 564.5–623.6 infl. p.–578.6	7.56 6.24	–	–
1.00	303.1–355.2 infl. p.–323.1	2.31	440.3–495.4 infl. p.–465.4	1.12	495.4–564.5 infl. p.–551.5 564.5–594.7 infl. p.–571.5	7.75 4.32	594.6–633.7 infl. p.–611.6	2.31
5.00	293.0–343.1 infl. p.–308.1	0.67	434.3–493.4 infl. p.–467.4	1.45	494.4–566.5 infl. p.–552.5 566.5–597.6 infl. p.–575.6	6.97 3.64	597.6–631.7 infl. p.–614.6	1.96

Table 3 Continued

Time of activation/h	Stage I		Stage II		Stage III		Stage IV	
	Temperature range/K	Mass loss/%	Temperature range/K	Mass loss/%	Temperature range/K	Mass loss/%	Temperature range/K	Mass loss/%
10.00	301.1–354.2 infl. p.–316.1	0.87	421.3–494.4 infl. p.–195.4	2.31	494.4–552.5 infl. p.–543.5 552.5–586.6 infl. p.–567.5	5.14 3.51	586.6–617.6 infl. p.–602.6	1.67
15.00	308.1–391.2 infl. p.–334.1	2.40	426.3–502.4 infl. p.–461.3	2.32	502.4–555.5 infl. p.–543.5 555.5–595.6 infl. p.–568.5	4.11 3.94	595.6–627.6 infl. p.–614.6	1.37
30.00	313.1–403.2 infl. p.–65.1	3.66	446.3–491.4 infl. p.–470.4	2.04	491.4–560.5 infl. p.–539.45 560.5–593.6 infl. p.–567.5	4.48 2.41	593.6–649.7 infl. p.–633.7	3.05
40.00	297.0–372.2 infl. p.–324.1	1.41	402.2–491.4 infl. p.–456.3	3.48	491.4–541.5 infl. p.–535.5 541.5–588.6 infl. p.–555.5	2.70 3.13	588.6–628.7 infl. p.–615.6	1.81
50.00	302.1–401.2 infl. p.–345.1	4.78	446.3–500.4 infl. p.–467.4	2.03	500.4–558.5 infl. p.–554.5 558.5–610.6 infl. p.–571.5	3.13 3.14	610.6–644.7 infl. p.–631.7	1.31

Table 3 Continued

Time of activation/h	Stage V		Stage VI		Stage VII		Total mass loss/%
	Temperature range/K	Mass loss/%	Temperature range/K	Mass loss/%	Temperature range/K	Mass loss/%	
0.00	670.7–706.8 infl. p.–696.8 706.8–788.9 infl. p.–717.8	9.92 8.48	883.1–1037.4 infl. p.–966.3	5.39	1037.4–1153.6 infl. p.–1096.5 1153.6–1273.8 infl. p.–1200.7	2.08 2.96	49.51
0.12	644.7–763.9 infl. p.–690.8	12.72	931.2–1011.3 infl. p.–974.3	2.91	1125.6–1240.8 infl. p.–1192.7	3.77	43.24
0.50	623.6–755.9 infl. p.–686.8	12.02	825.0–928.2 infl. p.–904.2 928.2–1001.3 infl. p.–954.2	2.91 2.74	1092.5–1158.6 infl. p.–1127.6 1158.6–1235.8 infl. p.–1189.7	1.83 2.91	46.50
1.00	633.7–730.8 infl. p.–677.7	9.76	876.1–991.3 infl. p.–946.2	4.32	1011.4–1148.6 infl. p.–1128.6 1148.6–1234.8 infl. p.–1196.7	2.35 3.43	44.10
5.00	631.7–677.7 infl. p.–668.7 677.7–746.9 infl. p.–693.8	3.84 4.74	824.0–905.2 infl. p.–860.1 905.2–988.3 infl. p.–926.2, 943.2	2.07 2.98	1069.5–1146.6 infl. p.–1121.5 1146.6–1196.7 infl. p.–1176.6 1196.7–1266.8 infl. p.–1219.7	2.03 2.19 3.09	39.66

Table 3 Continued

Time of activation/h	Stage V		Stage VI		Stage VII		Total mass loss/%
	Temperature range/K	Mass loss/%	Temperature range/K	Mass loss/%	Temperature range/K	Mass loss/%	
10.00	617.6–673.7 infl. p.–666.7 673.7–745.9 infl. p.–685.8	4.53 4.71	776.9–906.2 infl. p.–843.0 906.2–1032.4 infl. p.–935.2, 947.2	3.00 3.25	1032.4–1142.6 infl. p.–1119.5 1142.6–1205.7 infl. p.–1162.6	3.55 2.62	39.48
15.00	627.6–759.9 infl. p.–692.8	9.11	893.1–978.3 infl. p.–937.2	2.53	1045.4–1152.6 infl. p.–1129.6 1151.6–1180.7 infl. p.–1170.6 1180.7–1233.8 infl. p.–1190.69	2.98 1.68 1.75	38.62
30.00	649.7–751.9 infl. p.–689.8	6.49	897.1–997.3 infl. p.–936.1	2.04	1081.5–1162.6 infl. p.–1139.6 1162.6–1195.7 infl. p.–1167.6	4.84 1.28	36.83
40.00	628.7–737.9 infl. p.–678.7	7.60	841.0–903.2 infl. p.–887.1 903.2–972.3 infl. p.–929.2	1.32 1.20	1057.4–1143.6 infl. p.–1124.6 1143.6–1208.7 infl. p.–1156.6	4.20 2.98	35.69
50.00	644.7–737.9 infl. p.–687.8	6.012	737.9–886.1 infl. p.–558.0 886.1–999.3 infl. p.–941.2	1.93 1.13	1065.4–1136.6 infl. p.–1116.5 1136.6–1233.8 infl. p.–1177.6	2.04 5.21	34.25

infl. p.* – inflexed point

708–793 K, 8.49 mass loss/%

$$(NH_4)_3H(SO_4)_2=2NH_4HSO_4+NH_3 \tag{3}$$

$$(NH_4)_3H(SO_4)_2=(NH_4)_2S_2O_8+NH_3+H_2O \tag{4}$$

$$NH_4HSO_4=NH_3+SO_3+H_2O \tag{5}$$

883–1038 K, 5.39 mass loss/%

$$Ca_5F(PO_4)_3+NH_4CaP_3O_9=3Ca_2P_2O_7+HF+NH_3 \tag{13}$$

$$(NH_4)_2S_2O_8=2NH_3+2SO_3+H_2O+½O_2 \tag{6}$$

$$SO_3=SO_2+½O_2 \tag{7}$$

1093–1203 K, 5.10 mass loss/%

$$Ca_2P_2O_7+CaSO_4=Ca_3(PO_4)_2+SO_2+½O_2 \tag{14}$$

and/or

$$Ca_2P_2O_7+CaCO_3=Ca_3(PO_4)_2+CO_2 \tag{15}$$

$$CaCO_3=CaO+CO_2 \tag{16}$$

Triboactivated AS–TPh mixture

Data in Fig. 3 and Table 4 demonstrate the differences registered on the base of changes in the studied system during process of activation. The system is more sensitive during the first 60 min of treatment. The shape of TG-DTA curves and new solid structures, found by X-ray diffraction method, confirms that circumstance.

Diffractograms confirm that during the first 60 min of activation double salt $(NH_4)_2SO_4·2CaSO_4$ and $Ca_3(PO_4)_2·xH_2O$ are formed. So it is obvious that the local energy in the mixture makes possible transformations between main components in the system – $Ca_5F(PO_4)_3$ and $(NH_4)_2SO_4$. The same time release of NH_3 and SO_3 is confirmed.

When the time of activation increases to 5–15 h $(NH_4)_2H_2P_2O_7$, $NH_4CaP_3O_9$, $CaH_2P_2O_7$ and α-$Ca_2P_2O_7$ are registered in the mixture. Such solid phases are identified in the untreated mixture at very high temperatures. So it is obvious that activation energy is used for increasing the reactivity of the components in the studied system. When the time of activation is between 30 to 50 h intensities of $CaH_2P_2O_7$, α-$Ca_2P_2O_7$ and $NH_4CaP_3O_9$ are also confirmed, but the same time as new phases $CaSO_4·2H_2O$ and $Ca_3(PO_4)_2·xH_2O$ are formed. $(NH_4)_2H_2P_2O_7$ could not be detected by the X-ray study, but it is likely to be formed in the amorphous phase. At the same time it could be transformed to $CaH_2P_2O_7$ and α-$Ca_2P_2O_7$, according to reactions 17 and 18.

$$3(NH_4)_2H_2P_2O_7+2Ca_5F(PO_4)_3=4CaH_2P_2O_7+2HF+6NH_3+2Ca_3(PO_4)_2+H_2O \tag{17}$$

$$(NH_4)_2H_2P_2O_7+2Ca_5F(PO_4)_3=2Ca_2P_2O_7+2Ca_3(PO_4)_2+2HF+2NH_3+H_2O \tag{18}$$

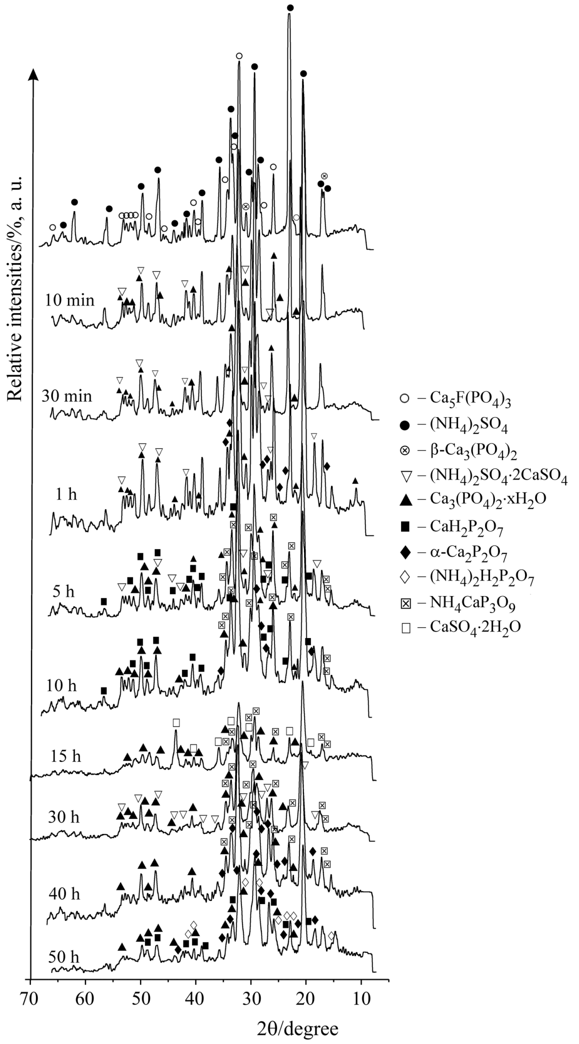

Fig. 3 X-ray diffraction patterns of the activated mixture

Formation of gypsum structures is another confirmation for the reactions between apatite structure and ammonium sulfate intermediates. TG curves show that by increasing the time of activation from 10 min to 50 h the mass losses decrease from 49.5 to 34.3% (Figs 4–6). It is another confirmation for the reactions taken place during activation process. At the same time the thermal effects characterizing reactions proceed are at lower temperatures by some 35 to 100 K. The differences are higher for high temperature transformations. For activated samples the new endo-effects at 323–348 and 493–563 K indicate the dehydration of formed $CaSO_4·2H_2O$ and the formation of the double salt $(NH_4)_2SO_4·2CaSO_4$ and $Ca_3(PO_4)_2·xH_2O$. Thermal effects are in a good agreement with mass changes registered.

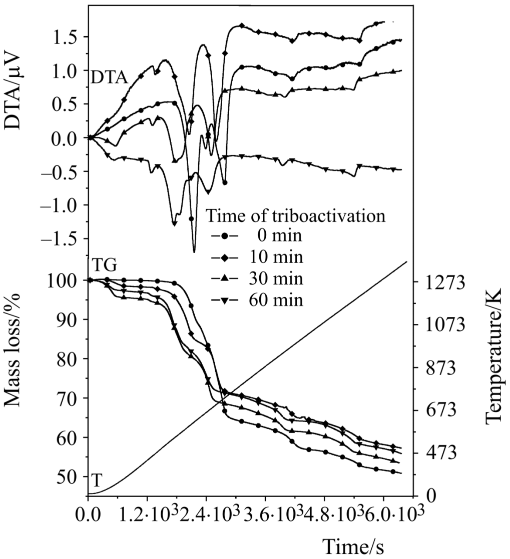

Fig. 4 TG-DTA curves of activated initial AS+TPh mixture; activation time –10 to 60 min

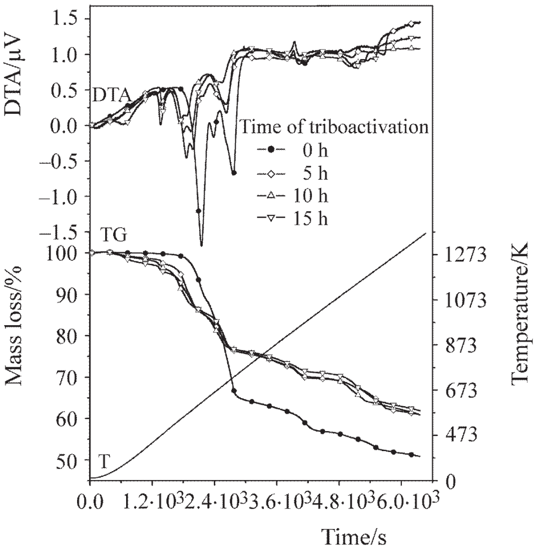

Fig. 5 TG-DTA curves of activated initial AS+TPh mixture; activation time –5 to 15 h

In the temperature range 663–723 K for the initial mixture 2 endothermic effects are typical, when for activated samples in most of the cases there is overlapping. It could be explained by the acceleration of the rate of decomposition of NH_4HSO_4 and $(NH_4)_3H(SO_4)_2$ as intermediates and formation of $(NH_4)_2H_2P_2O_7$, $CaH_2P_2O_7$, α-$Ca_2P_2O_7$ and $NH_4CaP_3O_9$ at lower temperatures. Reactions 17 and 18 partially represent this mechanism.

Table 4 Influence of the time of activation on the solid phases, identified by X-ray

Time of mechanoactivation	Identified solid phases
0 min	$Ca_5F(PO_4)_3$, β-$Ca_3(PO_4)_2$, $(NH_4)_2SO_4$
10 min	$Ca_5F(PO_4)_3$, $(NH_4)_2SO_4$, β-$Ca_3(PO_4)_2$, $Ca_3(PO_4)_2{\cdot}xH_2O$, $(NH_4)_2SO_4{\cdot}2CaSO_4$
30 min	$Ca_5F(PO_4)_3$, $(NH_4)_2SO_4$, β-$Ca_3(PO_4)_2$, $Ca_3(PO_4)_2{\cdot}xH_2O$, $(NH_4)_2SO_4{\cdot}2CaSO_4$
60 min	$Ca_5F(PO_4)_3$, $(NH_4)_2SO_4$, β-$Ca_3(PO_4)_2$, $Ca_3(PO_4)_2{\cdot}xH_2O$, $(NH_4)_2SO_4{\cdot}2CaSO_4$, α-$Ca_2P_2O_7$
5 h	$Ca_5F(PO_4)_3$, $(NH_4)_2SO_4$, β-$Ca_3(PO_4)_2$, $Ca_3(PO_4)_2{\cdot}xH_2O$, $(NH_4)_2SO_4{\cdot}2CaSO_4$, $(NH_4)_2H_2P_2O_7$, $CaH_2P_2O_7$, α-$Ca_2P_2O_7$, $NH_4CaP_3O_9$
10 h	$Ca_5F(PO_4)_3$, $(NH_4)_2SO_4$, β-$Ca_3(PO_4)_2$, $Ca_3(PO_4)_2{\cdot}xH_2O$, $CaH_2P_2O_7$, α-$Ca_2P_2O_7$, $NH_4CaP_3O_9$, $CaSO_4{\cdot}2H_2O$
15 h	$Ca_5F(PO_4)_3$, $(NH_4)_2SO_4$, β-$Ca_3(PO_4)_2$, $Ca_3(PO_4)_2{\cdot}xH_2O$, $(NH_4)_2H_2P_2O_7$, α-$Ca_2P_2O_7$, $NH_4CaP_3O_9$
30 h	$Ca_5F(PO_4)_3$, $(NH_4)_2SO_4$, $Ca_3(PO_4)_2{\cdot}xH_2O$, $CaH_2P_2O_7$, α-$Ca_2P_2O_7$, $NH_4CaP_3O_9$, $CaSO_4{\cdot}2H_2O$
40 h	$Ca_5F(PO_4)_3$, $(NH_4)_2SO_4$, $Ca_3(PO_4)_2{\cdot}xH_2O$, $CaH_2P_2O_7$, $NH_4CaP_3O_9$, $CaSO_4{\cdot}2H_2O$
50 h	$Ca_5F(PO_4)_3$, $(NH_4)_2SO_4$, $Ca_3(PO_4)_2{\cdot}xH_2O$, $CaH_2P_2O_7$, α-$Ca_2P_2O_7$, $CaSO_4{\cdot}2H_2O$

In the temperature range 843–943 K mass losses are only about 3%, but two thermal effects, one endothermic and one exothermic, are registered. The endother-

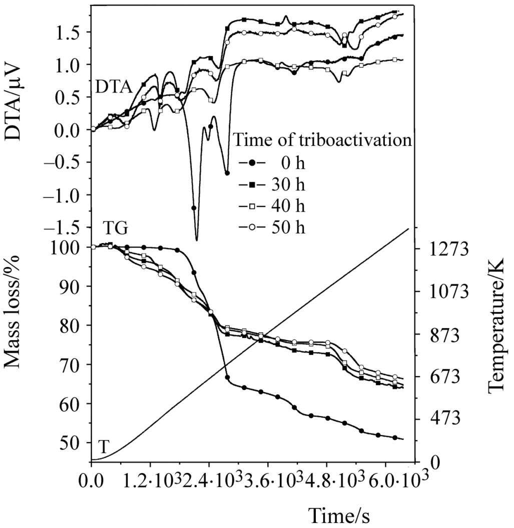

Fig. 6 TG-DTA curves of activated initial AS+TPh mixture; activation time –30 to 50 h

mic effect we understand as a transformation of $CaH_2P_2O_7$ to α-$Ca_2P_2O_7$ (reaction 19) and the releasing of some volatile impurities from TPh. Reaction 13 could also partially explain such an effect. The exothermic effect is observed only for activated samples and it could be just the relocation process of the crystal deformations.

$$CaH_2P_2O_7+Ca_3(PO_4)_2=2Ca_2P_2O_7+H_2O \tag{19}$$

The last stage changes are in the temperature range 973–1173 K and for untreated mixture it is due to the decomposition of the free CaO_3 from the natural phosphate. For activated samples it is the result of interaction between $CaSO_4$ and α-$Ca_2P_2O_7$.

Conclusions

New data for inactivated and activated mixture/ (activation time is from 0.12 to 50 h) of ammonium sulfate and Tunisia phosphorite is obtained. Thermal stability and behavior up to 1373 K confirm that during activation process different reactions are taking place and formation of new solid phases obtained, like $(NH_4)_2H_2P_2O_7$, $CaH_2P_2O_7$, α-$Ca_2P_2O_7$, $NH_4CaP_3O_9$ and $Ca_3(PO_4)_2$ is a fact. Such solid phases may appear after thermal treatment of the initial mixture at higher temperature. During activation process formation of the new solid phases demonstrate that the insoluble apatite phosphate structure could be transformed to other phosphorous compounds water or citric acid soluble, so the activation of such mixtures can be used in the practice for fertilizers production. Needed soluble forms could be obtained only after 10 min of treatment at lower temperatures and the impurities do not affect the process efficiency.

References

1 M. V. Chaikina, Chemistry for Sustainable Development, 41 (1996) 71.
2 A. Toneva and Jv. Dombalov, J. Balkan Tribological Association, 1–2 (1994) 149.
3 Iv. Dombalov, A. Toneva, J. Pelovski and Iv. Gruncharov, ‘Tribochemistry of sedimentary natural phosphates’, Proc. 1st International Conference on Mechanochemistry, March 23–26, Kosice-Slovakia 1993, p. 241.
4 A. Toneva, J. Pelovski and Jv. Dombalov, J. Thermal Anal., 43 (1995) 156.
5 Y. Pelovski and V. Petkova, J. Thermal Anal., 43 (1995) 339.
6 A. J. E. Welch, Proc. 2nd International Congress on Phosphorus Compounds Proceeding, 21–25 April, Boston 1980, USA, p. 363.
7 M. Marraha, M. Heughebart, G.-C. Heugbaert and G. Bonel, Biomat. Biomech., (1983) 445.
8 M. Veiderma, K. Tonsuaadu, M. Peld and V. Bender, Phosphorus Res. Bull., 10 (1990) 256.
9 M. Arasheva and Jv. Dombalov, J. Thermal Anal., 43 (1995) 359.
10 K. Tonsuaadu, M. Peld, V. Bender and M. Veiderma, J. Therm. Anal. Cal., 56 (1999) 35.
11 I. Dombalov, Y. Pelovski and V. Petkova, J. Therm. Anal. Cal., 56 (1999) 87.